P-ISSN: 2723-3863 E-ISSN: 2723-3871 Vol. 6, No. 5, October 2025, Page. 3445-3455

https://jutif.if.unsoed.ac.id

DOI: https://doi.org/10.52436/1.jutif.2025.6.5.4742

Brain Tumor Segmentation From MRI Images Using MLU-Net with Residual Connections

Eric Timothy Rompisa*1, Gede Putra Kusuma²

^{1,2}BINUS Graduate Program Master of Computer Science, Bina Nusantara University, Indonesia

Email: ¹eric.rompis@binus.ac.id

Received: May 16, 2025; Revised: Jul 1, 2025; Accepted: Jul 4, 2025; Published: Oct 16, 2025

Abstract

Brain tumor segmentation plays an important role in medical imaging in assisting diagnosis and treatment planning. Although advances in deep learning such as Unet already perform image segmentation, many challenges exist in segmenting brain tumors with tumor spread boundaries. This paper proposes a model that combines CNN and MLP (MLU-Net) techniques enhanced by the addition of residual connections to improve segmentation accuracy called ResMLU-Net. This architecture combines 2D covolution layers, block MLP and residual connections to process MRI images with the dataset used is BraTS 2021. The residual connection helps reduce gradient degradation which ensures smooth information flow and better feature learning. The performance of ResMLU-Net will be evaluated using Dice and IoU metrics and will also be compared with several models such as Unet, ResUnet and MLU-Net. The experimental scores obtained from ResMLU-Net for segmenting brain tumors are 83.43% for IoU and 89.94% for Dice. These results show that adding residual connections can improve the accuracy in segmenting brain tumors which can be seen that there is an increase in the Dice and Iou scores. The proposed ResMLU-Net model is a valuable contribution to medical imaging and health informatics. With its provision of a standard and computationally viable solution to brain tumor segmentation, it offers incorporation into Computer-Aided Diagnosis (CAD) systems and support to clinical decision-making protocols.

Keywords: Brain Tumor, CNN, Image Segmentation, Residual Connection, U-Net.

This work is an open access article and licensed under a Creative Commons Attribution-Non Commercial 4.0 International License



1. INTRODUCTION

Brain tumors are malignant cancers that develop within brain tissue. These tumors may originate from various cell types, either from the brain itself or from other tissues that have metastasized to the brain [1]. Brain tumors can be classified based on their histological characteristics, location, and malignancy grade [2]. Gliomas, originating from glial cells, are the most common type and account for the majority of cases. However, other tumor types such as meningiomas, medulloblastomas, and glioblastoma multiforme (GBM) are often more aggressive [3], [4]. Symptoms vary depending on tumor type, size, and location, and may include headaches, nausea, vomiting, vision problems, muscle weakness, and behavioral or mental changes [5]. Diagnostic tests to assist physicians include Magnetic Resonance Imaging (MRI), Computed Tomography (CT), biopsy, or surgery. Standard treatments generally involve a combination of surgery, chemotherapy, and radiotherapy. Prognosis largely depends on tumor type, location, disease stage, as well as the patient's age and overall health condition [6], [7]. Nevertheless, significant challenges remain in treating and understanding the complex pathophysiology of brain tumors. Consequently, ongoing research focuses on novel diagnostics, treatments, and innovative services aimed at improving early detection and treatment to enhance patient survival and quality of life [8].

The diagnostic process begins with an in-depth assessment of patient symptoms and medical history, followed by imaging studies such as MRI or CT scans to evaluate brain structure and detect

P-ISSN: 2723-3863 E-ISSN: 2723-3871 Vol. 6, No. 5, October 2025, Page. 3445-3455 https://jutif.if.unsoed.ac.id

DOI: https://doi.org/10.52436/1.jutif.2025.6.5.4742

tumor presence and type [9]. MRI provides highly detailed information about the brain's structural integrity and aids in reporting tumor size, location, and extent [10]. Tissue biopsy, involving removal of tumor samples for laboratory examination, remains one of the few definitive methods for confirming diagnosis and histology [11]. Additional diagnostic tools include positron emission tomography (PET) scans and angiography to assess tumor metabolic activity and blood flow in affected brain regions [12]. A comprehensive and precise diagnostic process is essential for establishing appropriate treatment plans tailored to patient needs. Despite advances in imaging and diagnostics, challenges persist in interpreting results and accurately identifying tumors, especially complex or rare brain tumors [13].

One of the critical steps in managing brain tumors is accurate image segmentation, which involves distinguishing, separating, and delineating tumor regions from normal brain structures in MRI images [14], [15]. This process facilitates visualization of tumor location and boundaries, enabling clinicians to plan treatment and monitor disease progression effectively, often with the support of deep learning-based segmentation models [16]. Segmentation models utilize computational algorithms to automate the identification and separation of tumor areas from MRI scans. Notably, artificial neural network architectures such as U-Net have demonstrated considerable potential in medical image segmentation [17]. The segmentation pipeline typically includes image preprocessing to enhance quality and contrast, feature extraction to detect salient characteristics, and clustering or classification to differentiate tumor regions from the background [18]. Automated segmentation often integrates multimodal MRI information (e.g., T1-weighted, T2-weighted, and FLAIR) to improve accuracy and reliability [19]. Despite these advances, accurately demarcating tumor regions in whole-brain images remains challenging, particularly for heterogeneous or occluded tumors. Hence, research and development in segmentation algorithms continue actively [20].

Deep learning, implemented through artificial neural networks, has revolutionized medical image segmentation and improved brain tumor detection methods [21]. These models analyze complex features in medical images, resulting in highly precise automated tumor detection and segmentation [22]. The U-Net architecture is pivotal in biomedical image segmentation due to its carefully crafted design, combining an encoder-decoder framework with skip connections that transfer information directly from encoder to decoder layers, thereby enhancing spatial feature learning [23]. The development of 3D convolutional neural networks (CNNs), incorporating volumetric spatial data, further improves segmentation precision [24]. Deep learning also facilitates transfer learning, leveraging pre-trained models on large datasets to enhance performance on medical datasets [25]. Although deep learning has significantly advanced brain tumor segmentation, the complex variability of medical images continues to challenge the maintenance of high model quality. Further research is needed to improve algorithmic performance through data integration, ultimately enhancing diagnostic accuracy and treatment efficacy [26].

Since its introduction by Ronneberger et al. in 2015, U-Net has become a primary framework for medical image segmentation, including brain tumor segmentation [23]. It is optimized to solve segmentation problems in biomedical imagery while preserving essential spatial information. The encoder extracts image features while the decoder reconstructs these features spatially. Its distinctive skip connections transmit data directly from encoder layers to corresponding decoder layers [27], enabling the simultaneous capture of detailed local features and broader global image patterns [28]. U-Net processes high-resolution images and preserves crucial anatomical details essential for segmentation tasks [29]. Due to its efficiency and success, U-Net is widely adopted in biomedical image processing, including brain tumor segmentation. However, it has limitations in capturing extensive and deep spatial features from images. Thus, continuous efforts in the medical imaging community aim to refine U-Net and develop improved versions to enhance segmentation accuracy and reliability in MRI brain tumor scans [30].

Vol. 6, No. 5, October 2025, Page. 3445-3455 https://jutif.if.unsoed.ac.id

DOI: https://doi.org/10.52436/1.jutif.2025.6.5.4742

Recent studies have proposed multiple models to enhance brain tumor segmentation accuracy and performance. ELU-Net improves U-Net by incorporating deep skip connections and combined loss functions for superior learning [17]. SGEResU-Net integrates a 3D U-Net architecture with residual blocks and spatial group enhancement (SGE) attention blocks to improve semantic feature accuracy [18]. SwinBTS combines 3D transformers with 3D CNNs and encoder-decoder structures to effectively capture contextual information [19]. TransU2-Net combines Transformer technology with U2-Net, stacking convolutional layers and transformers with skip connections to enhance both global and local information representation [20].

This research aims to enhance the U-Net-based MLU-Net architecture by integrating residual blocks, inspired by previous work combining residual learning with U-Net, known as ResUNet. This integration leverages the strengths of both architectures, facilitating the acquisition of more robust and informative feature representations. This approach addresses challenges in complex medical image processing and improves overall segmentation performance.

2. **METHOD**

E-ISSN: 2723-3871

2.1. **Research Stages**

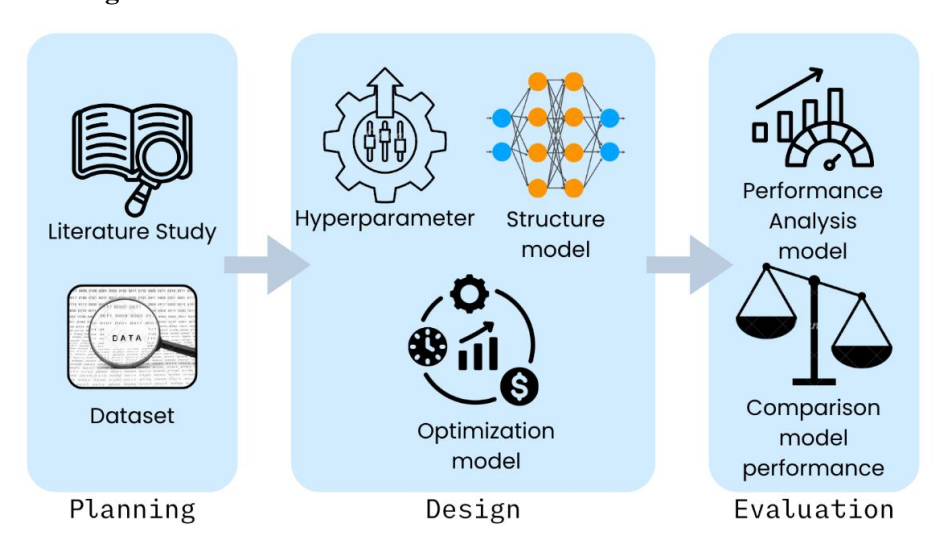


Figure 1. Research Stage

As shown in Figure 1, the research phases have explicit three elements: planning, design, and evaluation. Each element has a particular role in ensuring an image segmentation process is a success. Planning is the initial process of developing a research project. It is an essential realization of the research aim, available resources, and procedures for achieving the purpose. In image segmentation, planning may entail a proper survey of the literature so that the existing techniques would be known to us, in addition to planning for acquiring an appropriate dataset to train and test the model.

After the planning is complete, comes the design step. This is where the model or algorithm for a particular application, for instance, image segmentation, is formulated. Here it would involve formulating an artificial neural network model or employing other image segmentation techniques such as image-based techniques. It also involves selecting appropriate parameters, model structure, and data preprocessing techniques.

The evaluation step is where the performance of the model created is assessed. It is done through testing the model with the dataset already prepared. In image segmentation, it may involve metrics such as Intersection over Union (IoU) and Dice coefficient. The model created is compared against current models or other benchmark models to determine whether it provides a better performance.

https://jutif.if.unsoed.ac.id

DOI: https://doi.org/10.52436/1.jutif.2025.6.5.4742

2.2. Dataset

P-ISSN: 2723-3863

E-ISSN: 2723-3871

The BraTS 2021 dataset has been specifically designed to support research in brain tumor detection, segmentation, and characterization through medical imaging, particularly MRI (Magnetic Resonance Imaging). This dataset comprises MRI images from patients with brain tumors, encompassing various types such as T1-weighted, contrast-enhanced T1-weighted, T2-weighted, and FLAIR (Fluid Attenuated Inversion Recovery), along with segmentation data. For an example of a 2021 Brast image, as shown in Figure 2.

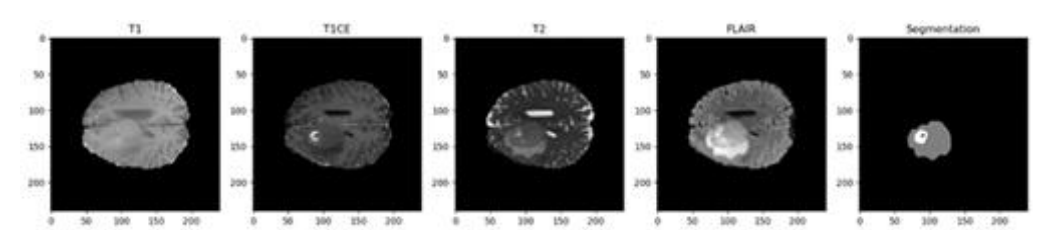


Figure 2. MRI Images BraTS 2021

Each image in the dataset is accompanied by annotations identifying various tumor-affected regions, including the tumor core, such as necrosis and solid tumor, peritumoral edema, and non-enhancing regions. Notable characteristics of the dataset include variations in data quantities across versions, substantial complexity in image structure and representation, and precise annotations to facilitate the development and validation of medical image processing algorithms. Consequently, the BraTS 2021 dataset offers researchers the opportunity to explore various aspects of brain tumor diagnosis, treatment, and prognosis through computational and medical approaches. Can be seen for the distribution of datasets in Table I.

 Dataset
 Amount of Image

 Train
 750

 Validation
 251

 Test
 251

Table 1. Dataset Distribution

2.3. Proposed Medel

The architecture of the Residual MLU-Net is depicted in Figure 3. The network takes the input of a medical image, which is processed layer-wise through a cascade of Conv2D layers with tenably 32, 64, 128, 256, and 512 filters. In these layers, the images are convoluted to extract salient features by detecting fundamental patterns, including edges, textures, and shapes. BatchNorm layers are applied to process the output of the convolutional layers and are smeared with rectified linear units (ReLU). Due to their non-linear nature, the ReLU activation functions could allow the model to learn more complicated representations. After convolution and activation, the model employs down-sampling through max pooling, which reduces the spatial dimensions of extracted features by a factor of 2 to preserve important information, in turn, reducing the parameters and computational costs in the network. This operation continues until features are selected at an increasing level of abstraction.

The remaining blocks are tokenized MLP (Multilayer Perceptron) cells. Frequency-based representations are embedded to obtain deeper associations among the features through MLP-based techniques. The next operation performed by the net is up-sampling, reaching its original resolution and achieving a higher resolution for more accurate and detailed segmentation. This is repeated to ensure that all salient features are retained.

P-ISSN: 2723-3863

E-ISSN: 2723-3871

DOI: https://doi.org/10.52436/1.jutif.2025.6.5.4742

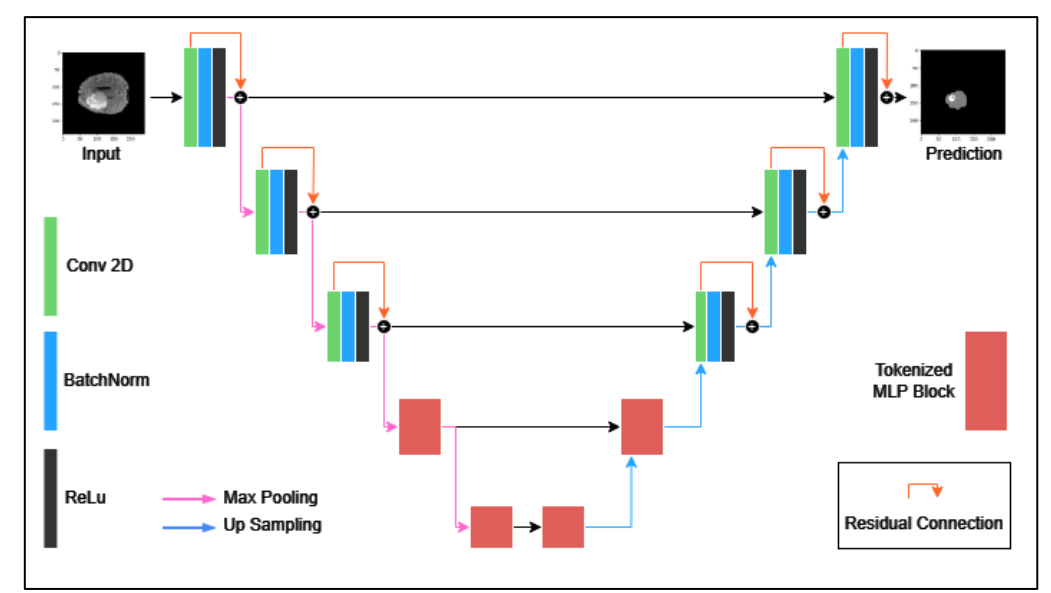


Figure 3. ResMLU-Net

Application of residual connections in this architecture permits the flow of information from the previous layers to the subsequent layers. The connections have been shown to overcome the issue of gradient degradation and enhance information flow, thereby enabling the network to learn more complex features. Moreover, residual connections have been shown to make the training of deep networks less complicated because they enable the gradients to pass through the network easily. The output of the model is the segmented image, and it's the network's prediction. The Dice and IoU are employed in an attempt to measure the goodness of the model. Dice computes prediction and ground truth similarity, and IoU computes prediction and ground truth overlap. Utilizing both of these two metrics provides an all-around assessment of the model's performance on image segmentation. Finally, the improved model performance is compared to that of the original MLU-Net model. This is indicated by the Dice and IoU scores, and the test results will indicate whether the incorporation of residual connections and tokenized MLP blocks significantly improves the performance of the model on processing large-scale data as well as on forming relationships between adjacent pixels.

2.4. Experimental Design

First, the image size used in training was 128x128 pixels, chosen to strike a balance between sufficient detail and computational efficiency. The batch size, which refers to the number of data samples used in one training iteration, was set to 16, taking into account the trade-off between training speed and model stability. The learning rate used was 0.001, carefully selected to avoid learning that is too slow or too fast. The optimizer employed was Adam. Lastly, the number of training iterations, or epochs, was set to 10, 20, and 30 epochs as part of the experimental process to evaluate the model's performance at various levels of complexity, as shown in Table 2.

Table 2. Hyperparameter Settings

Parameters	Unet	ResUnet	MLU-Net	ResMLU-Net				
Image size	128x128	128x128	128x128	128x128				
Batch size	1	1	1	1				
Learning rate	0.001	0.001	0.001	0.001				
Optimizer	Adam	Adam	Adam	Adam				
Epochs	30	30	30	30				

P-ISSN: 2723-3863 E-ISSN: 2723-3871

This phase begins with end-to-end training on a human brain MRI dataset using several models, namely U-Net, ResUnet, and ResMLPU-Net, to perform brain tumor segmentation. The implementation will be divided into three parts: training, validation, and testing. The implementation is carried out on Google Colab to run the code, which is written in Python. The primary library used is TensorFlow. Python is executed using a GPU since GPUs have more cores and are better suited for parallel data computation, making deep learning model training (CNN) faster on large datasets compared to CPUs. To use a GPU, CUDA and cuDNN need to be installed, but these are already available on Google Colab. Additionally, other libraries such as numpy, pandas, Keras, skimage, nilearn, and others are required for various Python modules. Scikit-learn is used for splitting the dataset into three parts: training, validation, and testing with a ratio of 60:20:20.

In the training and validation phases, the model is trained for 50 epochs, utilizing Keras callbacks with EarlyStopping so that training stops when the validation loss no longer decreases. This phase concludes by evaluating the performance on the validation stage. Afterward, the testing phase begins, where the trained models are tested using the test data. Models are tested by performing segmentation on prepared MRI images, and performance metrics, including loss, accuracy, and IoU, are displayed. For performance measurement on the Residual MLU-Net model, Dice and IoU metrics are used. These two measurements can serve as evaluation criteria for image segmentation. As can be seen in Equations (1) and (2).

$$Dice = \frac{2|Yp \cap Yt|}{|Yp| + |Yt|} = \frac{2TP}{FP + 2TP + FN} \tag{1}$$

$$IoU = \frac{|Yp \cap Yt|}{|Yp \cup Yt|} = \frac{TP}{TP + FP + FN}$$
 (2)

3. RESULT

3.1. Training and Validation

Next, experiments were conducted on the proposed model of this research, namely ResMLU-Net, using the same hyperparameters and dataset distribution as the previous experiments. The image size for training and validation was set to 256 x 256 pixels to maintain a balance between capturing adequate detail and optimizing computational efficiency. The batch size, representing the number of samples processed per training iteration, was chosen as 16 to balance training speed with model stability. A learning rate of 0.001 was selected to prevent overly slow or rapid learning. The optimizer used was Adam, and training was conducted for 30 epochs to assess the model's performance at different levels of complexity as part of the experimental process.

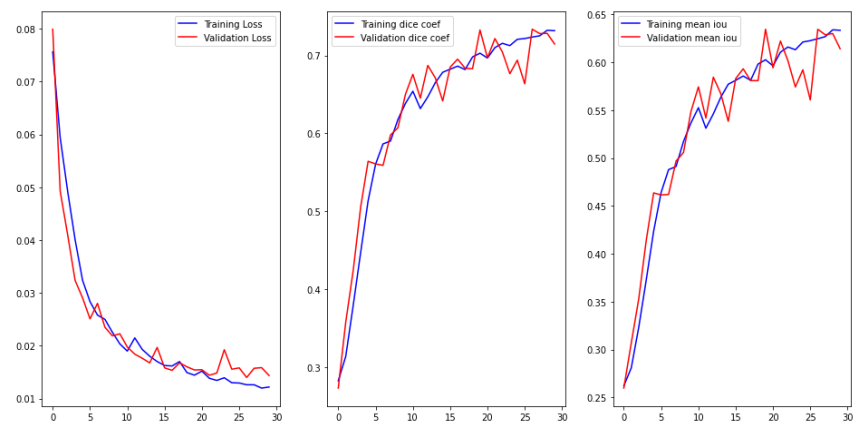


Figure 4. ResMLU-Net Training and validation Result

DOI: https://doi.org/10.52436/1.jutif.2025.6.5.4742

P-ISSN: 2723-3863 E-ISSN: 2723-3871

The training and validation results of ResMLU-Net are shown in the plots in Figure 4. In the first plot, both the training loss and validation loss exhibit a stable decrease, with values remaining close to each other, indicating no significant signs of overfitting. The second plot shows a consistent increase in the Dice coefficient for both the training and validation data, demonstrating that the model is becoming more accurate in the segmentation task. Meanwhile, in the third plot, the mean IoU initially fluctuates but then shows an upward trend and stabilizes, with the training and validation values becoming increasingly aligned. For the training and validation results of the 4 models can be seen in Table 3.

Table 5. Training and variation result							
Metriks		Unet	ResUnet	MLU-Net	ResMLU-Net		
Loss	Training	1.69	1.58	1.73	1.27		
	Validasi	1.63	1.59	1.92	1.19		
Dice	Training	80.22%	84.01%	84.26%	85.74%		
	Validasi	81.47%	85.10%	83.34%	86.39%		
IoU	Training	79.03%	80.25%	80.14%	81.29%		
	Validasi	80.04%	82.38%	81.17%	82.71%		

Table 3. Training and Validation Result

3.2. Testing

The segmentation results demonstrate that the model successfully performed the segmentation task, particularly in distinguishing tumor areas from other parts of the brain. When comparing the segmentation results with the Ground Truth, the ReU-Net and ResMLU-Net models showed a very high degree of similarity, with predictions almost identical to the Ground Truth. This indicates that both models were able to accurately identify and separate the tumor areas with high precision. On the other hand, the U-Net model still exhibited some prediction errors, where certain areas did not align with the Ground Truth, indicating that this model was less accurate in segmentation compared to ReU-Net and ResMLU-Net. The segmentation results can be seen in Figures 5-7.

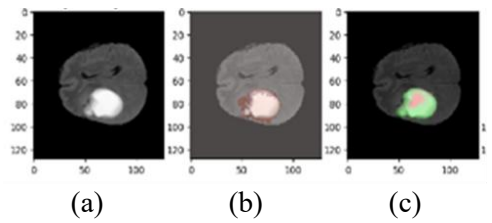


Figure. 5 (a) Original image (b) Ground truth (c) Unet segmentation results

In Figure 5, (a) is the original image of the data and (b) is the ground truth, which is an image manually segmented by experts and will be the reference for comparison with the prediction results. For image (c) is the segmentation result of the Unet model. It can be seen that the experiments with the Unet model produce a segmentation that covers a good part of the tumor, but there are still parts that are not included in the prediction segmentation results.

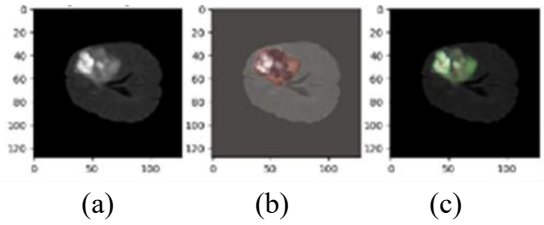


Figure 6. (a) Original image (b) Ground truth (c) ResUnet segmentation results

P-ISSN: 2723-3863

E-ISSN: 2723-3871

DOI: https://doi.org/10.52436/1.jutif.2025.6.5.4742

The results of the experiment conducted using ResUNet are presented in Figure 6. It can be observed that the comparison of the ground truth with the prediction results obtained using the ResUNet model demonstrates a relatively effective segmentation of some of the unpredicted ground truth.

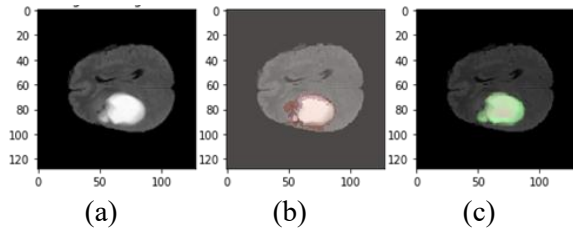


Figure 7. (a) Original image (b) Ground truth (c) MLU-Net segmentation results

Moreover, Figure 7 depicts the outcome of the experiment utilizing the MLU-Net model. It is evident that the comparison between the ground truth (b) and the prediction results (c) produced by the MLU-Net model exhibits a relatively high degree of accuracy, with the exception of a portion of the ground that was not predicted. The MLU-Net model has been previously tested for segmentation with other data sets, demonstrating excellent performance. However, when applied to more complex datasets, its performance has exhibited a decline.

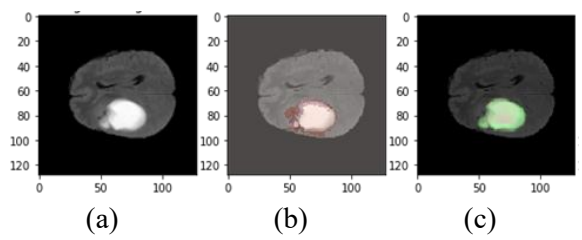


Figure 8. (a) Original image (b) Ground truth (c) ResMLU-Net segmentation results

With the use of the same hyperparameters for all models, the performance differences are clearly due to the architecture used. The addition of residual blocks to the U-Net and MLU-Net models has been proven to improve stability and optimize training duration, ultimately resulting in better performance in brain tumor segmentation tasks. And the proposed model ResMLU-Net provides optimal segmentation results. As can be seen the results of brain tumor segmentation using ResMLU-Net in Figure 8.

In the final stage, testing was conducted using the testing dataset for all four models. The results can be seen in Table 4.

Model	Loss	IoU	Dice
Unet	1.62	79.9%	83.47%
ResUnet	1.59	82.51%	87.88%
MLU-Net	2.26	81.90%	82.87%
ResMLU-Net	1.52	83.43%	89.94%

4. DISCUSSIONS

Adding residual connections to the U-Net architecture, forming ResU-Net, yielded a dramatic improvement in segmentation results, as evident from an increase in the Intersection over Union (IoU) score from 79.9% to 82.51%, and the Dice coefficient from 83.47% to 87.88%. The same pattern was observed in the case of MLU-Net. When residual connections were incorporated to construct ResMLU-

Jurnal Teknik Informatika (JUTIF)

P-ISSN: 2723-3863 E-ISSN: 2723-3871 Vol. 6, No. 5, October 2025, Page. 3445-3455 https://jutif.if.unsoed.ac.id

DOI: https://doi.org/10.52436/1.jutif.2025.6.5.4742

Net, the IoU score also improved significantly from 81.90% to 83.43%, and the Dice score improved from 82.87% to 89.94%. These results indicate that residual learning is useful for feature representation and segmentation precision. In addition, the loss value of ResMLU-Net was minimized to 1.52, compared to 2.26 in the baseline MLU-Net, which represents increased training stability and a lower prediction error rate.

These findings show the superiority of residual connections in boosting the performance of segmentation models. Relative to ELU-Net [17], whose Dice score on this dataset was 87.11%, ResMLU-Net was superior at a Dice score of 89.94%. In a similar fashion, SGEResUNet [18], which uses spatial group enhancement blocks, achieved a Dice score of 88.12%, which was inferior to that of ResMLU-Net. This is proof of the robustness of residual-enhanced architectures for learning advanced features. The IoU accuracy of ResMLU-Net at 83.43% is also comparable with SwinBTS [26], which is a Transformer-based model but with high cost of computation for high accuracy. This means that ResMLU-Net offers a fair compromise between efficiency and accuracy.

The proposed ResMLU-Net model is a valuable contribution to medical imaging and health informatics. With its provision of a standard and computationally viable solution to brain tumor segmentation, it offers incorporation into Computer-Aided Diagnosis (CAD) systems and support to clinical decision-making protocols.

5. CONCLUSION

In this study, it was demonstrated that the addition of residual blocks to the U-Net (ReU-Net) significantly improved the performance of tumor segmentation. The increase in IoU values pointed towards ReU-Net as superior to the baseline U-Net and previous studies while distinguishing between tumor regions and normal brain tissue. The segmentation performance of ResMLU-Net has also improved in the same way on adding residual blocks due to the increase in IoU values, thus indicating its efficiency in accurate discrimination of tumor areas and neighboring tissues.

These models were satisfactorily evaluated against the BraTS2021 dataset, whereby ReU-Net and ResMLU-Net distinguish tumor regions with good accuracy. More advanced hardware should thus be utilized in the future, with higher computational power to hasten the process of model training and inference, leading to the optimal inferences that can be achieved. Moreover, changes in preprocessing, such as better data normalization techniques and augmentation methods, can be further refined while tailoring specific characteristics of the dataset in question to further improve model performance. They also suggest finding alternative architectures/methodologies, including attention mechanisms or transfer learning, to improve segmentation precision.

REFERENCES

- [1] C. S. Muir, H. H. Storm, and A. Polednak, "Brain and other nervous system tumours," Cancer Surveys. [Online]. Available: https://www.cancer.gov/types/brain
- [2] D. N. Louis *et al.*, "The 2021 WHO classification of tumors of the central nervous system: A summary," *Neuro Oncol*, vol. 23, no. 8, pp. 1231–1251, 2021, doi: 10.1093/neuonc/noab106.
- [3] I. B. L. M. Suta, R. S. Hartati, and Y. Divayana, "Diagnosa Tumor Otak Berdasarkan Citra MRI (Magnetic Resonance Imaging)," *Majalah Ilmiah Teknologi Elektro*, vol. 18, no. 2, 2019, doi: 10.24843/mite.2019.v18i02.p01.
- [4] P. Cranston, "Brain Tumor," The journal of pastoral care & counseling: JPCC. [Online]. Available: https://www.mayoclinic.org/diseases-conditions/brain-tumor/symptoms-causes/syc-20350084
- [5] M. F. Safdar and S. S. Alkobaisi, "A comparative analysis of data augmentation approaches for magnetic resonance imaging (MRI) scan images of brain tumor," *Acta Informatica Medica*, vol. 28, no. 1, pp. 29–36, 2020, doi: 10.5455/aim.2020.28.29-36.

Jurnal Teknik Informatika (JUTIF)

Vol. 6, No. 5, October 2025, Page. 3445-3455 P-ISSN: 2723-3863 https://jutif.if.unsoed.ac.id E-ISSN: 2723-3871 DOI: https://doi.org/10.52436/1.jutif.2025.6.5.4742

[6] B. K. Ahir, H. H. Engelhard, and S. S. Lakka, "Tumor development and angiogenesis in adult brain tumor: Glioblastoma," Int J Mol Sci, vol. 21, no. 20, pp. 2461-2478, 2020, doi: 10.3390/ijms21204648.

- Y. He et al., "Automatic left ventricle segmentation from cardiac magnetic resonance images [7] using a capsule network," J Xray Sci Technol, vol. 28, no. 3, pp. 541-553, 2020, doi: 10.3233/XST-190621.
- T. Akan, A. G. Oskouei, and S. Alp, "Brain magnetic resonance image (MRI) segmentation using [8] multimodal optimization," Multimed Tools Appl, 2024, doi: 10.1007/s11042-024-19725-4.
- [9] U. Baid and others, "The RSNA-ASNR-MICCAI BraTS 2021 benchmark on brain tumor segmentation and radiogenomic classification," arXiv preprint, 2021, [Online]. Available: http://arxiv.org/abs/2107.02314
- A. Younis, L. Qiang, C. O. Nyatega, M. J. Adamu, and H. B. Kawuwa, "Brain tumor analysis [10] using deep learning and VGG-16 ensembling learning approaches," Applied Sciences, vol. 12, no. 2, pp. 1–14, 2022, doi: 10.3390/app12020689.
- O. Ronneberger and T. Fischer, P., & Brox, "U-Net: Convolutional Networks for Biomedical [11] Segmentation," ArXiv, vol. arXiv:1505, 2015, [Online]. https://arxiv.org/abs/1505.04597
- [12] R. Budi, R. A. Harianto, and E. Setyati, "Segmentasi citra area tumpukan sampah dengan memanfaatkan Mask R-CNN," Journal of Intelligent System and Computation, vol. 5, no. 1, pp. 58-64, 2023, doi: 10.52985/insyst.v5i1.305.
- Y. Xie, J. Zhang, and C. Shen, "CoTr: Efficiently bridging CNN and transformer for medical [13] image segmentation," arXiv preprint, 2021.
- H. Huang and others, "UNet 3+: A full-scale connected UNet for medical image segmentation," [14] in Proc. IEEE Int. Conf. Acoustics, Speech and Signal Processing (ICASSP), 2020, pp. 1055– 1059. doi: 10.1109/ICASSP40776.2020.9053405.
- R. Azad, M. Asadi-Aghbolaghi, M. Fathy, and S. Escalera, "Medical image segmentation [15] review: The success of U-Net," Pattern Recognit, vol. 128, pp. 1-38, 2022, doi: 10.1016/j.patcog.2022.108675.
- M. K. Anbudevi and K. Suganthi, "Review of semantic segmentation of medical images using [16] modified architectures of UNET," J Healthc Eng, vol. 2022, pp. 1-11, 2022, doi: 10.1155/2022/8423073.
- [17] Y. Deng, Y. Hou, J. Yan, and D. Zeng, "ELU-Net: An efficient and lightweight U-Net for medical image segmentation," IEEE Access, vol. 10, pp. 35932-35941, 2022, doi: 10.1109/ACCESS.2022.3163711.
- D. Liu and others, "SGEResU-Net for brain tumor segmentation," Mathematical Biosciences [18] and Engineering, vol. 19, no. 6, pp. 5576–5590, 2022, doi: 10.3934/mbe.2022261.
- X. Li and others, "TransU2-Net: An effective medical image segmentation framework based on [19] transformer and U2-Net," IEEE J Transl Eng Health Med, vol. 11, pp. 441-450, 2023, doi: 10.1109/JTEHM.2023.32899990.
- [20] L. Feng and others, "MLU-Net: A multi-level lightweight U-Net for medical image segmentation integrating frequency representation and MLP-based methods," IEEE Access, vol. 12, pp. 20734-20751, 2024, doi: 10.1109/ACCESS.2024.3360889.
- [21] F. I. Diakogiannis, F. Waldner, P. Caccetta, and C. Wu, "ResUNet-a: A deep learning framework for semantic segmentation of remotely sensed data," ISPRS Journal of Photogrammetry and Remote Sensing, vol. 162, pp. 94–114, 2020, doi: 10.1016/j.isprsjprs.2020.01.013.
- D. Zhang and others, "Cross-modality deep feature learning for brain tumor segmentation," [22] Pattern Recognit, vol. 110, pp. 1–10, 2021, doi: 10.1016/j.patcog.2020.107562.
- [23] P. Wang and A. C. S. Chung, "Relax and focus on brain tumor segmentation," Med Image Anal, vol. 75, p. 102259, 2021, doi: 10.1016/j.media.2021.102259.
- Y. Zhang and others, "mmFormer: Multimodal medical transformer for incomplete multimodal [24] learning of brain tumor segmentation," in Lecture Notes in Computer Science, vol. 13435, 2022, pp. 107–117. doi: 10.1007/978-3-031-16443-9 11.

Jurnal Teknik Informatika (JUTIF)

Vol. 6, No. 5, October 2025, Page. 3445-3455 P-ISSN: 2723-3863 https://jutif.if.unsoed.ac.id E-ISSN: 2723-3871 DOI: https://doi.org/10.52436/1.jutif.2025.6.5.4742

- Z. Xing and others, "NestedFormer: Nested modality-aware transformer for brain tumor [25] segmentation," in Lecture Notes in Computer Science, vol. 13435, 2022, pp. 140-150. doi: 10.1007/978-3-031-16443-9 14.
- Y. Jiang and others, "SwinBTS: A method for 3D multimodal brain tumor segmentation using [26] Swin Transformer," *Brain Sci*, vol. 12, no. 6, pp. 1–15, 2022, doi: 10.3390/brainsci12060797.
- F. Ullah and others, "Brain tumor segmentation from MRI images using handcrafted [27] convolutional neural network," Diagnostics, vol. 13, no. 16, pp. 1-15, 2023, doi: 10.3390/diagnostics13162650.
- M. Vatanpour and J. Haddadnia, "TransDoubleU-Net: Dual scale Swin Transformer with dual [28] level decoder for 3D multimodal brain tumor segmentation," *IEEE Access*, vol. 11, pp. 125511– 125518, 2023, doi: 10.1109/ACCESS.2023.3330958.
- J. Lin and others, "CKD-TransBTS: Clinical knowledge-driven hybrid transformer with [29] modality-correlated cross-attention for brain tumor segmentation," IEEE Trans Med Imaging, vol. 42, no. 8, pp. 2451–2461, 2023, doi: 10.1109/TMI.2023.3250474.
- T. Magadza and S. Viriri, "Efficient nnU-Net for brain tumor segmentation," *IEEE Access*, vol. [30] 11, pp. 126386–126397, 2023, doi: 10.1109/ACCESS.2023.3329517.